

Country neighborhood network on territory and its geometrical model

Qi Xuan* and Tie-Jun Wu

Department of Control Science and Engineering, Zhejiang University, Hangzhou 310027, China

(Received 17 October 2008; revised manuscript received 2 March 2009; published 17 April 2009)

The country neighborhood network, where nodes represent countries and two nodes are considered linked if the corresponding countries are neighbors on territory, is created and its giant component, the Asia, Europe, and Africa (AEA) cluster, is carefully studied in this paper. It is found that, as common, the degree distribution and the clustering function of the AEA cluster are both compatible with scale-free property, besides, the AEA cluster presents a little disassortativity, and its near power-law country area-degree relationship with the exponent close to 1.7 may imply a fractal dimension close to 1.2 of country borderlines in the AEA continent. It is also revealed that the average difference of population density between two countries obeys an approximately increasing function of the shortest path length between them, which may suggest a gradual consensus of population density in the AEA cluster. A simple unity rule is then adopted to model the AEA cluster and such model explains the AEA cluster very well in most aspects, e.g., power-law domain area distribution and fractal domain borderlines, etc., except that the network derived by the model has stronger disassortativity, which may be explained by the fact that, in the evolution history of countries, unbalanced neighbors are more likely to be united as one than balanced neighbors. Additionally, the network evolving process can be divided into three periods, defined as formation period, growth period, and combination period, and there are indications that the AEA cluster is in its third period.

DOI: [10.1103/PhysRevE.79.046106](https://doi.org/10.1103/PhysRevE.79.046106)

PACS number(s): 89.75.Hc, 89.75.Da, 89.75.Fb, 05.45.Df

I. INTRODUCTION

Nowadays, more and more complex systems in various areas, e.g., sociology [1–3], technology [4–6], and biology [7,8], are described as complex networks. Interestingly, many of them share some similar network properties [9,10], e.g., scale-free property $P(k) \sim k^{-\gamma}$ characterizing a very heterogeneous degree distribution and power-law clustering function $C(k) \sim k^{-\beta}$ suggesting a hierarchical and modular structure in some situations [7,8,11,12]. Scale-free networks [1,9–14] are always modeled by adopting the preferential attachment (PA) and the growth rules first proposed by Barabási and Albert [1]. Of course, such scale-free property also can be derived by other mechanisms. For instance, Newman *et al.* [15] provided a statistical mechanism to generate random networks with arbitrary degree distributions. Caldarelli *et al.* [16] presented a fitness model, where each node is associated with a fitness, and such model could generate power-law degree distributions for various fitness distributions and attaching rules. Recently, Xuan *et al.* [17] pointed out that compelled cooperation in the networks lack of resources could be another way to such heterogeneous degree distribution. Meanwhile, the power-law clustering function can be easily explained by introducing local-world restrictions into the complex network models [12–14].

More or less, the evolutions of many real-world complex networks are influenced by many geographical factors, and the most direct factor may be the partition of the administrative organizations, e.g., countries, provinces, cities, villages and so on [12]. In fact, many worldwide complex networks, such as worldwide trade network [3], worldwide routing net-

work [4], international air transportation network [5], and so on, are attached on the basic layered worldwide network, i.e., country neighborhood network (CNN), where nodes represent countries and two nodes are considered linked if the corresponding countries are neighbors on territory. In the same way, those nationwide complex networks [6] may also be attached on the province neighborhood network, and so on. Studying this type of geographical networks is of much importance not only because they determine the structure of many other complex networks attached on them for a certain extent, but also with the reason that understanding the evolutions of these geographical networks itself has its notable sociological significance, e.g., natural population migration as well as the consequent convention and religion communications always occurs between linked (neighborhood) countries.

In this paper, the world map [18,19] is transferred to the CNN, and the Asia, Europe and Africa (AEA) continent and the America continent form the top two largest clusters in the CNN. Experiential studies show that both the AEA cluster and the America cluster have no small-world property just because they have quite long average shortest path length $\langle L \rangle$ for their relatively small size although both of them have much large average clustering coefficient $\langle C \rangle$. Furthermore, it seems that the degree distribution and the clustering function of the giant component of the CNN are both compatible with scale-free property, which is consistent with many other reported complex networks [9,10], although the evidence is not so sufficient due to the small number of nodes in the AEA cluster. At the same time, the AEA cluster presents a little disassortativity [9,10]. Besides, the formation of countries on the AEA continent can be generalized to a surface partition problem which is also of many physical interests [20,21]. In this paper, it is shown that the country area distribution, as well as the relationship between the area of a country and the degree of the corresponding node, also pre-

*Author to whom correspondence should be addressed; crestxq@hotmail.com

sents a scale-free property, and the power-law exponent of the latter is close to 1.7, a little smaller than 2, may imply a fractal dimension close to $2/1.7=1.2$ of country borderlines in the AEA continent. Coincidentally, the coastline of the Africa was also found to possess a fractal dimension close to 1.2 [22]. More interestingly, the average difference of population density between two countries obeys an approximately increasing function of the shortest path length between them may suggest a gradual consensus [23] of population density in the AEA cluster.

Although lots of existing network models can explain these properties very well [8,9,11–14], they cannot exhibit the reasonable evolution mechanism of the CNN. The GeoSim model [24] can simulate the evolution of countries of many details, however, it seems too complicated with a network view to be theoretically analyzed and generalized to other related areas. In fact, with the improvement of the technology and the spread of the civilization, unity, other than division or growth, dominates the AEA continent in the history and hence is adopted to model the CNN in this paper. Thus the principle of our model is very simple, while the resulting network derived by the model indeed has similar properties as those of the AEA cluster, i.e., large average clustering coefficient, similar degree distribution and clustering function, power-law domain area distribution, and fractal domain borderlines. Besides, the average difference of area between two domains also obeys a similar approximately decreasing function of the shortest path length between them. However, the network derived by the model has much smaller average shortest path length than the AEA cluster, which is mainly because the model does not take the complex geographical condition of the AEA continent into account. The fact is that Africa is connected to Asia and Europe through a narrow chain, composed by Egypt, Israel, Palestine, Jordan, Lebanon, Syria, and Iraq, which must largely increase the average shortest path length of the AEA cluster. Further analysis shows that the whole evolving process of the model can be divided into three periods, i.e., formation period, growth period, and combination period, where the network behaves totally different. Also the existence of the large area countries, e.g., Russia and China, in the AEA continent may suggest that the AEA cluster is in its combination period.

Based on the fact that unity happens frequently in many real-world complex systems, the modeling mechanism provided in this paper can be generalized to model many other real-world complex networks in higher dimensional evolving spaces. For example, the model can successfully explain the power-law file size distribution through a positive feedback mechanism: the neighboring files, i.e., sharing similar topics, ideas, or contents, are more likely to be united in the future, and the larger size of the united file will allow it to hold more neighboring files, and so forth, which is very similar to the *multiplicative process* introduced by Mitzenmacher [25]. The rest of the paper is organized as follows. In Sec. II, the country neighborhood network is provided and several of its properties are calculated. A simple model for the CNN based on the principle of unity is then proposed in Sec. III, where several properties of a network derived by the model, with similar size as that of the AEA cluster, are calculated to be

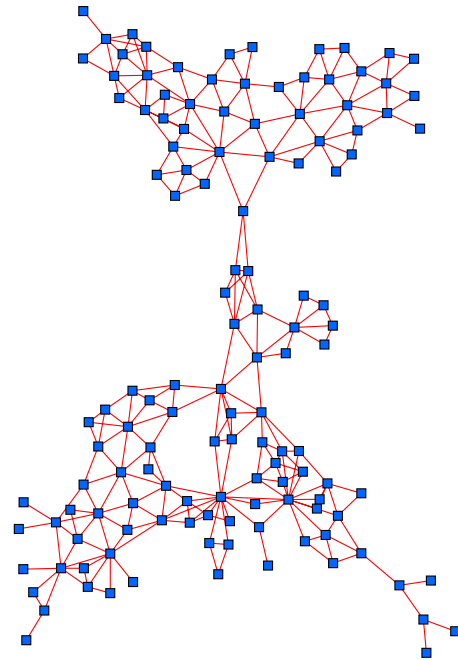


FIG. 1. (Color online) The structural map of the AEA cluster in the CNN.

compared with those of the AEA cluster. In Sec. IV, the model is analyzed both numerically and theoretically. Finally, the work is summarized in Sec. V.

II. EXPERIENTIAL ANALYSIS OF THE CNN

There are lots of countries having no neighbors on territory, i.e., Japan, England, and most countries in the Oceania. In fact, these single countries may indeed have neighbors if considering their marginal sea, which, however, does not belong to the scope of this paper. With the reason that the AEA continent and the America continent are the top two largest continents and at the same time form the top two largest clusters in the CNN, they are selected to be studied in this paper.

The AEA continent contains 130 countries (single countries, e.g., islands, are excluded). So the largest cluster of the CNN, named as AEA cluster, has 130 nodes, similarly, the America cluster has 24 nodes. Their structural maps are shown in Fig. 1 and Fig. 2, respectively. Meanwhile, some

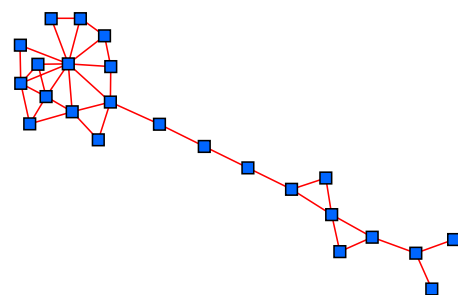


FIG. 2. (Color online) The structural map of the America cluster in the CNN.

classical network properties, i.e., the number of nodes N , the number of edges E , the average degree $\langle k \rangle$, the average clustering coefficient $\langle C \rangle$, and the average shortest path length $\langle L \rangle$, of these two clusters are summarized in Table I, where it is shown that both of these two clusters have no small-world property just because they have quite long average shortest path length $\langle L \rangle$ for their relatively small size although both of them have much large average clustering coefficient $\langle C \rangle$.

Because the AEA cluster evolves in a low-dimensional space ($d=2$) and contains a tiny number of nodes ($N=130$), its maximum node degree is quite small, i.e., $k_{\max}=14$. As a result, there will be little evidence to claim that some distribution related to degree k follows a certain distribution form, though it seems that the degree distribution $P(k)$ of the AEA cluster shown in Fig. 3(a) is indeed compatible with the scale-free property, which is coincident with many other worldwide complex networks [3–5]. The AEA cluster shown in Fig. 3(b) is lightly disassortative, suggesting that the nodes with similar degree are a little more unlikely to be connected with each other in the AEA cluster.

The clustering function $C(k)$ of the AEA cluster denoting the average clustering coefficient C on the nodes with degree k , shown in Fig. 3(c), is also compatible with the scale-free property, i.e., $C(k) \sim k^{-\beta}$. Power-law clustering function is

TABLE I. Several classical network properties, i.e., the number of nodes N , the number of edges E , the average degree $\langle k \rangle$, the average clustering coefficient $\langle C \rangle$, and the average shortest path length $\langle L \rangle$, of the AEA cluster, the America cluster, and the network derived by the model with parameters $n=40$ and $T=1470$.

Clusters	N	E	$\langle k \rangle$	$\langle C \rangle$	$\langle L \rangle$
AEA	130	276	4.25	0.52	6.70
America	24	38	3.17	0.49	4.49
Model	130	308	4.74	0.54	4.41

always considered to suggest a hierarchical and modular structure in many other real-world complex networks [7,8,11,12], in the CNN, however, such characteristic will be given another more visually explanation based on its geometrical essence. In fact, averagely speaking, in a d -dimensional Euclidean space, the neighbors of a domain will be arranged around its surface in order, as is shown in Fig. 4. So intuitively, the number of links between the neighbors of a node i , defined as e_i , will be directly proportional to its degree k_i . Then the clustering coefficient of the node i can be calculated by Eq. (1),

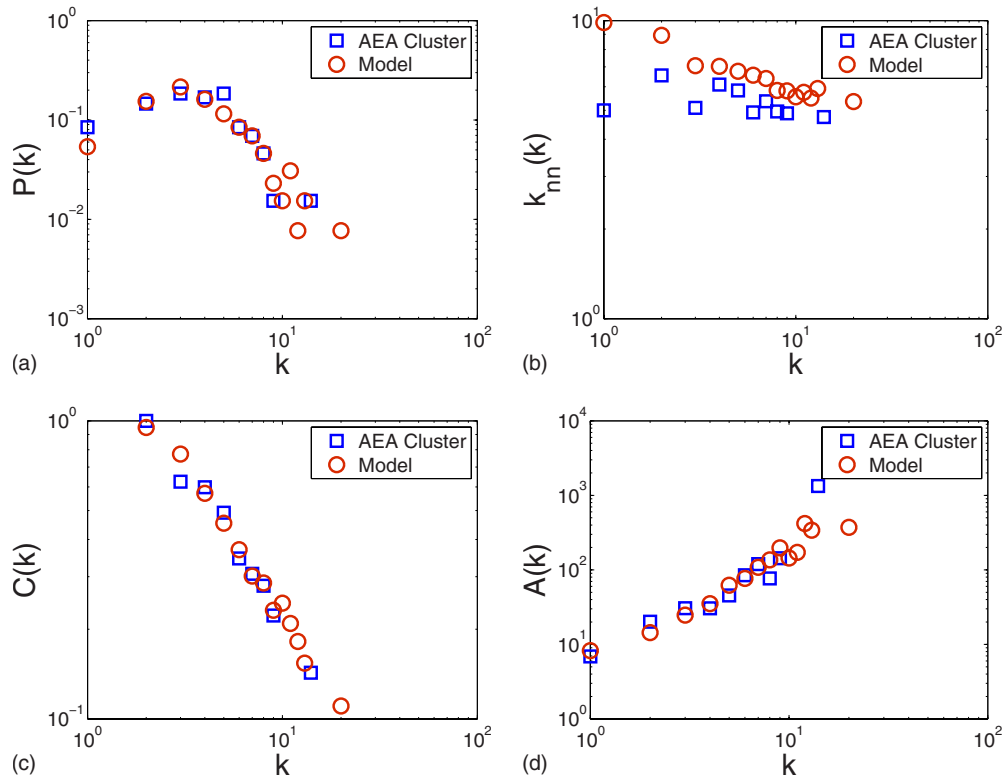


FIG. 3. (Color online) (a) The degree distributions, (b) the degree correlation functions, (c) the clustering functions, and (d) the country (domain) areas as the functions $A(k)$ (10^4 km^2) of the degree k for the AEA cluster in the CNN as well as the network derived by the model with the same number of nodes, i.e., the parameters of the model are set to be $n=40$ and $T=1470$. It should be noted that, in order to better compare with the AEA cluster, the square in the model is considered to have the same area as the AEA continent, i.e., the sum of the areas of all the 130 countries equaling to about $8375.9 (10^4 \text{ km}^2)$. The model fits the real data very well almost everywhere except that the network derived by the model presents a little more disassortativity than the AEA cluster.

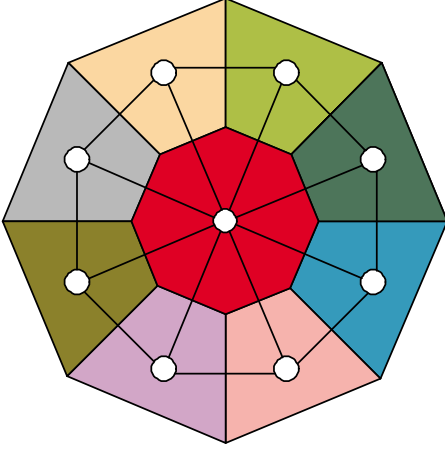


FIG. 4. (Color online) A depiction to describe the relationship between the local clustering coefficient $C(k_i)$ of a node i and its degree k_i .

$$C(k_i) = \frac{2e_i}{k_i(k_i - 1)} \sim \frac{k_i}{k_i(k_i - 1)} \sim \frac{1}{k_i}, \quad (1)$$

which indeed possesses a scale-free property with the absolute value of the power-law exponent $\beta=1$.

Statistically, in a d -dimensional Euclidean space, the relationship between the volume V_i and the surface area S_i of a domain (node) i always follows Eq. (2),

$$V_i^{1/d_v} \sim S_i^{1/d_s}, \quad (2)$$

where d_s denotes the fractal dimension of the surface and d_v denotes the fractal dimension of the volume satisfying that $d_s \leq d_v \leq d$ [22]. For the AEA cluster discussed in this paper, each country and even the AEA continent are both space filling, i.e., $d_v = d = 2$ must be satisfied. Then it can be expected that, in the AEA cluster, although there is slight degree correlation between nodes, the relationship between the area A_i of country i and the degree k_i of the corresponding node follows Eq. (3),

$$A_i \sim B_i^{2/d_s} \sim k_i^\alpha, \quad (3)$$

where the exponent is $\alpha = 2/d_s$ with the fractal dimension $d_s \in (1, 2)$ of the borderline. In fact, such relationship between the country area and node degree in the AEA cluster is shown in Fig. 3(d) and almost satisfies $A(k) \sim k^\alpha$ with the exponent $\alpha = 1.7$. This finding may inversely suggest that, statistically, the fractal dimension of country borderlines in the AEA continent is close to 1.2.

Besides these network characteristics, each node in the AEA cluster, as a country, has its nonstructural properties [19], e.g., area, population density, and so on. It is also very interesting to study the network correlations of these nonstructural properties, e.g., to reveal if two linked nodes possess similar areas or similar population densities. Denoting the difference of area between two nodes i and j by $D_A(i, j) = |A(i) - A(j)|$, the difference of population density between two nodes i and j by $D_{PD}(i, j) = |PD(i) - PD(j)|$, then the average difference of area between linked nodes or nonlinked nodes and the average difference of population

density between linked nodes or nonlinked nodes can be calculated by Eqs. (4)–(7), respectively,

$$D_A^1 = \frac{1}{N_E} \sum_{i=2}^N \sum_{j=1}^{i-1} D_A(i, j) E(i, j), \quad (4)$$

$$D_A^0 = \frac{2}{N(N-1) - 2N_E} \sum_{i=2}^N \sum_{j=1}^{i-1} D_A(i, j) [1 - E(i, j)], \quad (5)$$

$$D_{PD}^1 = \frac{1}{N_E} \sum_{i=2}^N \sum_{j=1}^{i-1} D_{PD}(i, j) E(i, j), \quad (6)$$

$$D_{PD}^0 = \frac{2}{N(N-1) - 2N_E} \sum_{i=2}^N \sum_{j=1}^{i-1} D_{PD}(i, j) [1 - E(i, j)], \quad (7)$$

where N_E represents the number of links in the AEA cluster, and $E(i, j) = 1$ if nodes i and j are linked while $E(i, j) = 0$ otherwise. In the AEA cluster, $D_A^1 = 179.5(10^4 \text{ km}^2) \gg D_A^0 = 92.4(10^4 \text{ km}^2)$ indicates that countries with larger difference of area are more likely to be linked, which is consistent with the disassortative property of the AEA cluster, while $D_{PD}^1 = 148.9(\text{person}/\text{km}^2) \ll D_{PD}^0 = 428.4(\text{person}/\text{km}^2)$, however, suggests that linked countries have closer population densities than those of nonlinked countries, which may be caused by the similar policies, conventions, and religions, as well as the natural population migration, between the linked countries.

Moreover, the average difference of area and the average difference of population density between two nodes with the shortest path length equal to L can be calculated by Eq. (8) and Eq. (9), respectively,

$$D_A(L) = \frac{1}{N_L} \sum_{i=2}^N \sum_{j=1}^{i-1} D_A(i, j) E_L(i, j), \quad (8)$$

$$D_{PD}(L) = \frac{1}{N_L} \sum_{i=2}^N \sum_{j=1}^{i-1} D_{PD}(i, j) E_L(i, j), \quad (9)$$

where N_L represents the number of pairs of nodes with the shortest path length equal to L , and $E_L(i, j) = 1$ if the shortest path length between the nodes i and j is equal to L while $E_L(i, j) = 0$ otherwise. Then the network correlations of areas and population densities of countries could be presented more quantitatively in Figs. 5(a) and 5(b), where it is shown that longer shortest path length between two countries always means a smaller difference of area but a larger difference of population density between them. More interestingly, in these two figures, it is clearly shown that $D_A(L)$ and $D_{PD}(L)$ both behave abnormally when $7 \leq L \leq 11$, unfortunately, there still lacks a reasonable explanation for such phenomenon. At the same time, it should be noted that the values of $D_A(L)$ and $D_{PD}(L)$ are less reliable when $L > 14$ because there are only a very small number of pairs of countries with the shortest path length larger than 14.

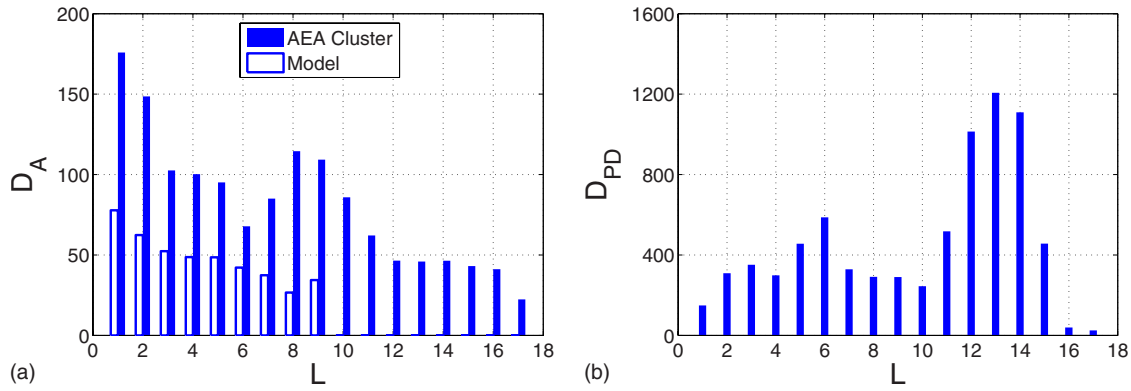


FIG. 5. (Color online) (a) The average difference of area between two nodes, i.e., $D_A(L)$ (10^4 km^2), as a function of the shortest path length equal to L between them for the AEA cluster in the CNN as well as the network derived by the model with the same number of nodes, i.e., the parameters of the model are set to be $n=40$ and $T=1470$. Similarly, the square in the model is considered to have the same area as the AEA continent. (b) The average difference of population density between two nodes, i.e., $D_{PD}(L)$ (person/ km^2), as a function of the shortest path length equal to L between them for the AEA cluster in the CNN.

III. MODEL

The evolution of countries in the world could be modeled by a specific multiagent system, i.e., the GeoSim model [24], of many details. For example, a country in the GeoSim model contains two different types of provinces, i.e., a capital and other normal provinces, and the complex resource allocation and competition mechanism determines the result of the warfare between two neighbored countries, then territorial changes occur, i.e., a country may win or lose one or more provinces, which may further lead to a structural change in the CNN. Such a detailed model could well explain some special events in the human history, e.g., power-law war-size distribution [24]. However, the complicated mechanism also makes it difficult to be theoretically analyzed and generalized to other related areas.

In the GeoSim model, the increment (decrement) of territory always means the focused country gains more neighbors (loses some of its neighbors), as a result, when the structure of the CNN is mainly focused in this paper, the modeling process of the GeoSim model could be remarkably simplified with a network view [17]. More macroscopically, as an immemorial aphorism says “being united for long must be divided, and being divided for long must be united” [26], the evolution of the CNN could be modeled by two simple operators, i.e., unity and division. Moreover, as the improvement of the technology and the spread of the civilization, unity dominates the AEA continent historically, e.g., Chinese history shows a continuously evolution with national unity as the dominant power from Spring and Autumn Period time (BC 770–476) to Qing dynasty (1616–1912) [27], i.e., although the country experienced three social divisions in history, it eventually moved toward Qin, Han, Sui, Tang, Yuan, Ming, and Qing unifications with an approximately increment of territory. Therefore, in this paper, we would like to propose a general network model for CNN just by adopting the principle of the second part of the aphorism. Different from the GeoSim model, such a simple network model not only can explain most of the statistical properties of the AEA cluster very well, but also can be easily generalized to ex-

plain the similar phenomena, e.g., the power-law file size distribution, in other areas. The modeling process is introduced as follows:

(i) Initialization: a square is divided into $n \times n$ grids, as is shown in Fig. 6(a), named as domains in this paper. With a network view, as is shown in Fig. 6(b), each domain is represented by a node, and two nodes are linked if their corresponding domains are neighbors.

(ii) Unity: at each time, a domain is randomly selected as the hot domain, and one of its neighbors is randomly selected as the affected domain, then they are united as one domain. With the network language, that is, the total number of the nodes in the network will decrease by 1, and the new node will possess all the neighbors that its parents (the nodes representing the hot domain and the affected domain) have had.

(iii) Termination: after T times, the process is terminated. For example, with the initial states presented in Fig. 6, after $T=80$ times uniting, the resulting domains and the corresponding network are shown in Figs. 7(a) and 7(b), respectively, where the grids marked the same number belongs to the same domain.

To get a network with the similar size as that of the AEA cluster, the parameters of the model are set to be $n=40$ and $T=1470$, then the number of nodes in the resulting network will be $N=130$. The structure of the resulting network with 130 nodes and 308 links is shown in Fig. 8, and some of its statistical characteristics are presented in Table I. Comparing the AEA cluster and the network derived by the model in Table I, it can be found that they are very similar on almost all of these structural properties except the average shortest path length $\langle L \rangle$, i.e., the average shortest path length of the network derived by the model is much smaller than that of the AEA cluster. This exception is mainly because the initial network in the model is a regular two-dimensional lattice without taking the complex geographical condition of the AEA continent into account. In fact, the world map clearly shows that Africa is connected to Asia and Europe through a narrow chain, composed of Egypt, Israel, Palestine, Jordan, Lebanon, Syria, and Iraq, which is reflected in Fig. 1, and such special geographical condition for sure largely increases

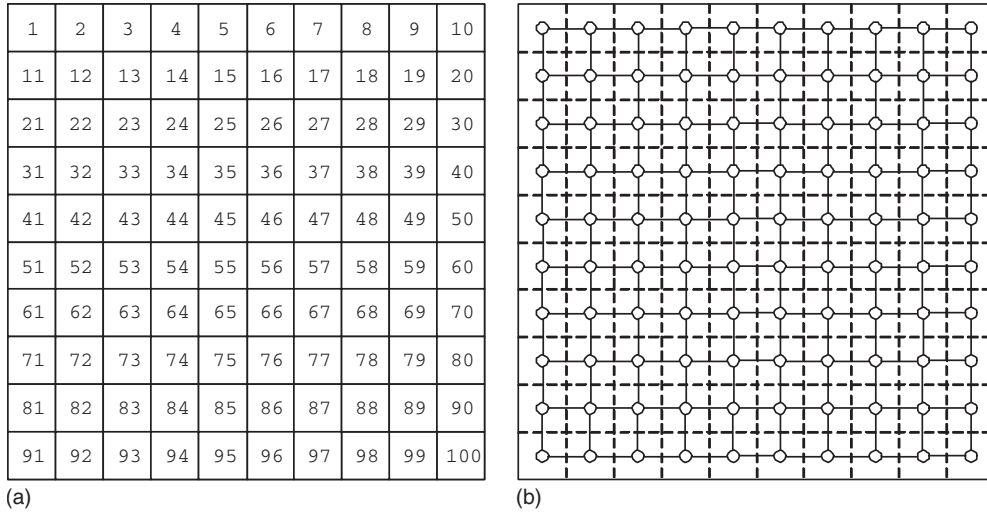


FIG. 6. (a) A square is divided into 10×10 domains. (b) The corresponding network where each domain is represented by a node and two nodes are linked if their corresponding domains are neighbors.

the average shortest path length $\langle L \rangle$ of the AEA cluster.

Furthermore, the network derived by the model has similar degree distribution, clustering function, and domain area-degree relationship [the area of a grid in the model is set to be $8375.9/1600=5.2(10^4 \text{ km}^2)$ in order to better compare with the AEA cluster] as those of the AEA cluster, as is shown in Figs. 3(a), 3(c), and 3(d), respectively. At the same time, as is in the AEA cluster, the average difference of area between two domains derived by the model obeys a similar approximately decreasing function of the shortest path length between them, which is shown in Fig. 5. The only exception is that the network derived by the model presents a little more disassortativity than the AEA cluster, as is shown in Fig. 3(b), and a reasonable explanation of such exception may be that, in the evolution history of countries, unbalanced neighbors are always more likely to be united as one than balanced neighbors. With a network language, in a more pre-

cise CNN model, the unity probability of the two linked nodes should be proportional to the gap between their degrees (or their domain areas), which, not adopted in this model, obviously can largely reduce the disassortativity of the network.

Computer simulations also show that the small maximum degree of the AEA cluster is mainly caused by its quite low-dimensional evolving space ($d=2$), as we can see in Fig. 9, the maximum degrees of the networks derived by the model with various $n=40, 50, 60, 70$ at different evolving phases $\tau = T/n^2$ keep a relatively low level, i.e., $k_{\max} < 35$, all the time, and there lacks of evidence that this value will increase as the grid scale $\delta=1/n$ is further reduced. Naturally, considering that the network evolving in the one-dimensional space has the maximum degree strictly equaling to 2, which is even much smaller than that of the network evolves in the two-dimensional space, it will be logical to infer that the model

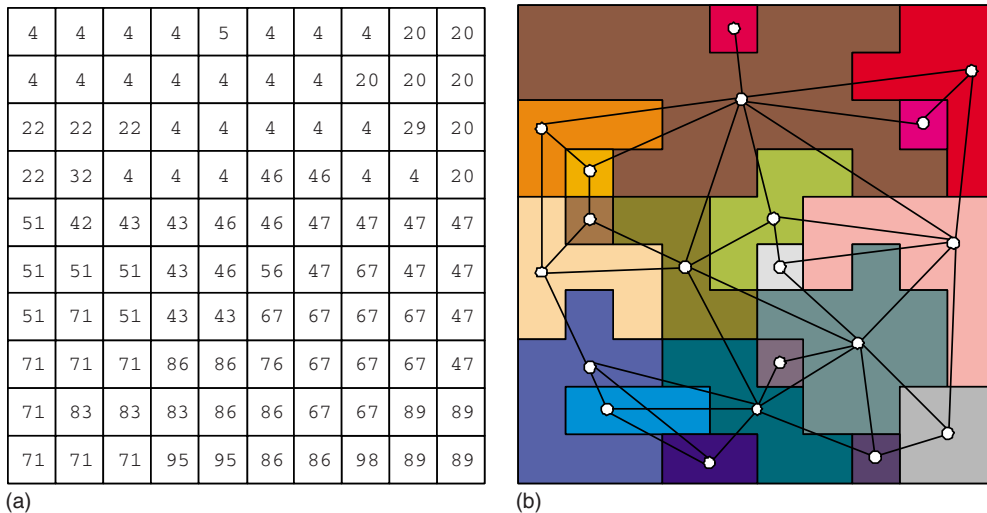


FIG. 7. (Color online) (a) The domains after $T=80$ times uniting, the grids marked by the same number belongs to the same domain. (b) The corresponding network, where each domain is represented by a node and two nodes are linked if their corresponding domains are neighbors.

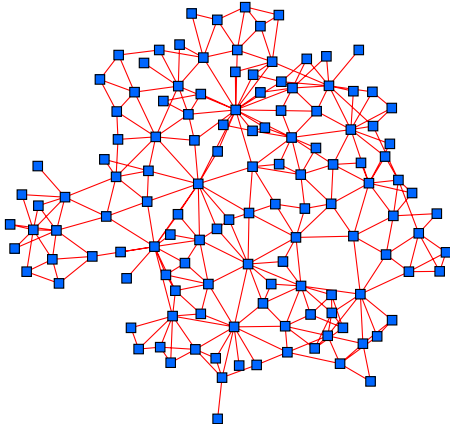


FIG. 8. (Color online) The structural map of the network derived by the model with parameters $n=40$ and $T=1470$.

can explain the power-law distributions more appropriately in a higher dimensional evolving space.

The country area distribution on the AEA continent also presents a scale-free property, described by Eq. (10),

$$P(A > S) \sim -\eta \ln S \Rightarrow P(A) \sim \eta A^{-1}, \quad (10)$$

after excluding the countries with extra small area less than $1 (10^4 \text{ km}^2)$, and this property can be well explained by the model through selecting appropriate grid scale $\delta=1/n$, i.e., $n=70$, as is shown in Fig. 10. Meanwhile, in order to better understand the fractal essence of the country borderlines, the relationship between the number N_δ of line segments with length δ needed to cover the domain borderlines of the network with a fixed number $N=130$ of nodes derived by the model and the grid scale $\delta=1/n$ is presented in Fig. 11. The power-law function $N_\delta \sim \delta^{-1.3}$ in this figure suggests that the domain borderlines of the networks derived by the model have fractal dimension close to 1.3 as long as the grid scale δ is sufficiently small. This value is very close to the fractal dimension of the country borderlines on the AEA continent calculated by Eq. (3).

IV. MODEL ANALYSIS

The modeling process introduced in the last section shows that the structure of the resulting network derived by the

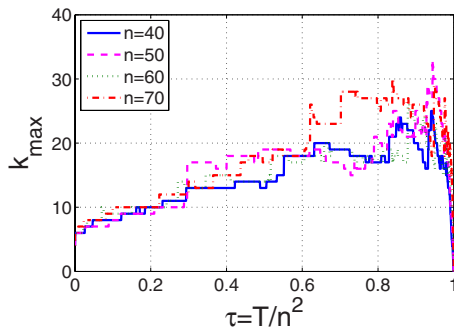


FIG. 9. (Color online) The maximum degrees k_{\max} of the networks derived by the model with various $n=40, 50, 60, 70$ at different evolving phases $\tau=T/n^2$.

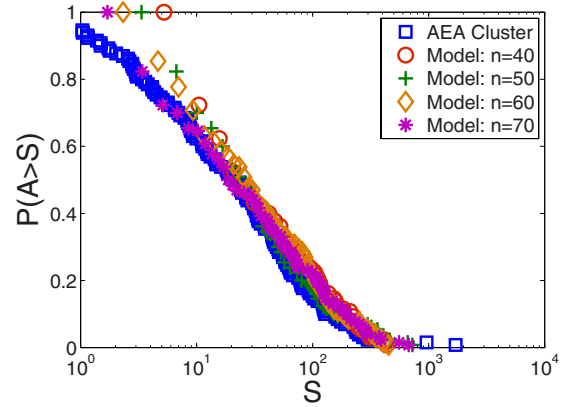


FIG. 10. (Color online) The domain (country) area cumulative distributions for the AEA cluster excluding the countries with area less than $1 (10^4 \text{ km}^2)$ and the four networks derived by the model with different parameters $n=40, 50, 60, 70$ and $T=1470, 2370, 3470, 4770$, respectively, as a result, these networks have the same number of nodes, i.e., $N=130$. Similarly, the total area of the square in the model is set to be $8375.9 (10^4 \text{ km}^2)$. All of these cumulative distributions follow $P(A > S) \sim -\eta \ln S$ suggesting that the domain area distributions of these networks possess the same scale-free property, i.e., $P(A) \sim \eta A^{-1}$.

model can be influenced by three parameters, i.e., the dimension d of the evolving space, the size n of the initial lattice, and the evolving time T . For example, the average degree $\langle k \rangle$ will be much larger and the average shortest path length $\langle L \rangle$ will be much shorter in an evolving space with higher dimension d . The network structural properties will be greatly changed as the network evolves (at different evolving time T), e.g., as is shown in the last section, compared with the initial lattice, the resulting network has totally different structural properties and the size n of the initial lattice must be large enough to present the whole evolving process.

Although all of these three parameters are needed to determine a network in the model, the evolving time T seems to be the key factor to the structural properties of the resulting

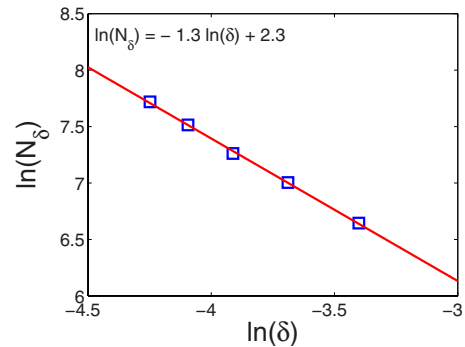


FIG. 11. (Color online) The number N_δ of line segments with length δ needed to cover the domain borderlines of the network with a fixed number N of nodes derived by the model as a function of the grid scale $\delta=1/n$. To compare with the AEA cluster, the number of nodes (domains) is set to be $N=130$, and the power-law function $N_\delta \sim \delta^{-1.3}$ shown in this figure suggests that the domain borderlines of the networks derived by the model have fractal dimension close to 1.3 as long as the grid scale δ is sufficiently small.

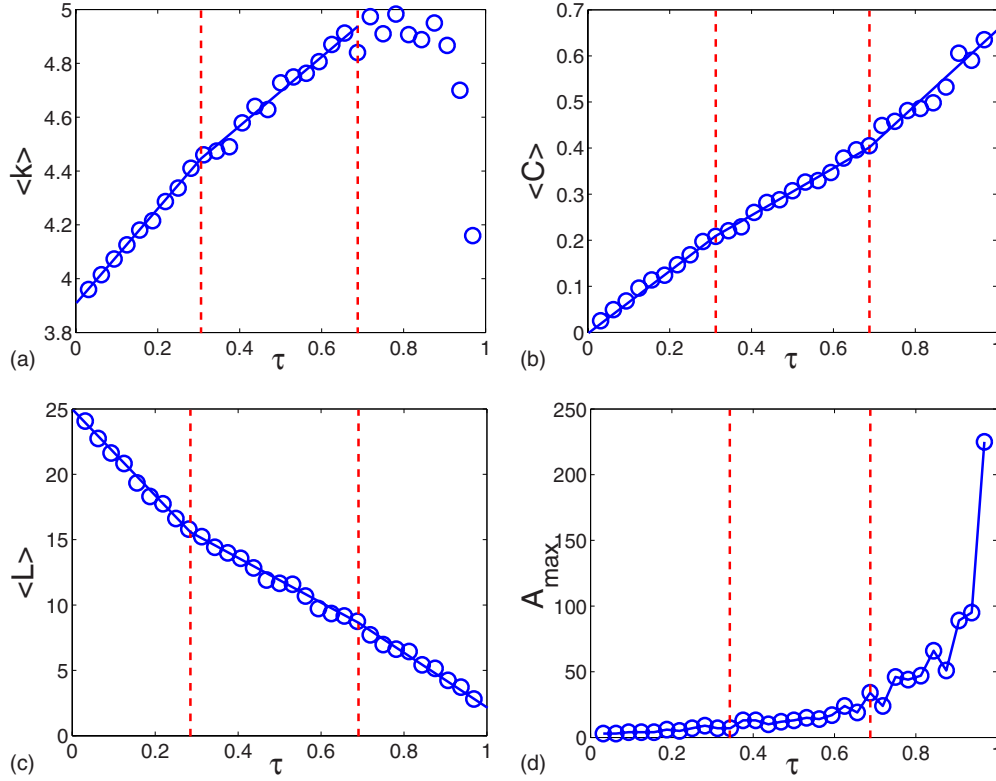


FIG. 12. (Color online) The trends of several network statistical properties as the network evolves where the evolving time T is normalized by $\tau=T/n^2$ denoting the phase of the evolving process. (a) The trend of the average degree $\langle k \rangle$ as the network evolves. (b) The trend of the average clustering coefficient $\langle C \rangle$ as the network evolves. (c) The trend of the average shortest path length $\langle L \rangle$ as the network evolves. (d) The trend of the maximum domain area A_{\max} as the network evolves. Each figure is divided into three sections, denoting formation period, growth period, and combination period, respectively, from left to right, by two vertical dash lines.

network. So in this section, the dimension d of the evolving space and the size n of the initial lattice are both fixed, and we mainly focus on the changes of the structural properties of the networks at different evolving time.

As the network evolves, the trends of several network statistical properties, i.e., the average degree $\langle k \rangle$, the average clustering coefficient $\langle C \rangle$, the average shortest path length $\langle L \rangle$, and the maximum domain area A_{\max} are shown in Figs. 12(a)–12(d), respectively, where $\tau=T/n^2$ denotes the phase of the evolving process. By analyzing these trends and reviewing the modeling details, it is found that there are three prominent periods divided by two critical points, i.e., $\tau_1 \approx 0.3$ and $\tau_2 \approx 0.7$, in the evolving process of the network. The three periods, respectively, named as formation period, growth period, and combination period are described as following three subsections.

A. Formation period ($\tau < \tau_1$)

In this beginning period, there are lots of minimum grid cells in the square, as is shown in Fig. 6(a), so in this period, lots of domains with small area but larger than the minimum grid cell will be formed by uniting these minimum grid cells, and naturally, there lacks of domains with large area, as is shown in Fig. 12(d), and the average maximum domain area of the networks in this period is close to 5.

In this period, the average degree $\langle k(t) \rangle$ at evolving time t approximately satisfies Eq. (11),

$$(N_0 - t)\langle k(t) \rangle \approx (N_0 - t + 1)\langle k(t - 1) \rangle - 2, \quad (11)$$

with the reason that always only one link disappears when unity happens at each time in this period. Equation (11) then can be easily transformed to a differential equation as Eq. (12),

$$\frac{d\langle k \rangle}{dt} \approx \frac{\langle k \rangle - 2}{N_0 - t}, \quad (12)$$

with the initial state $\langle k(0) \rangle \approx 4$. Then the trend of the average degree $\langle k \rangle$ as the network evolves can be calculated by Eq. (13),

$$\langle k \rangle \approx 2 + \frac{2N_0}{N_0 - t} = 2 + \frac{2}{1 - \tau}. \quad (13)$$

When τ is much smaller, Eq. (13) can be approximated by Eq. (14),

$$\langle k \rangle \sim 2 + 2(1 + \tau) = 4 + 2\tau. \quad (14)$$

Equation (14) shows that the average degree $\langle k \rangle$ will approximately linearly increase with the rate close to 2 as the

network evolves, which is verified by the numerical simulation shown in Fig. 12(a) with a little smaller rate close to 1.8.

Similarly, in this period, with the reason that the total increment of the clustering coefficient in a lattice at each time close to $4 \times 1/6 + 2/15 = 0.8$, the differential equation of the average clustering coefficient $\langle C \rangle$ can be approximated by Eq. (15),

$$\frac{d\langle C \rangle}{dt} \approx \frac{\langle C \rangle + 0.8}{N_0 - t}. \quad (15)$$

Then the trend of the average clustering coefficient $\langle C \rangle$ as the network evolves can be approximated by Eq. (16),

$$\langle C \rangle \approx \frac{0.8}{1 - \tau} - 0.8 \sim 0.8\tau, \quad (16)$$

which is verified by the numerical simulation shown in Fig. 12(b) with a little smaller increasing rate close to 0.65.

Statistically, each node in a regular lattice can be a part of the shortest paths between vast pairs of other nodes. As a result, in this period, the unity of two randomly selected linked nodes will obviously dramatically decrease the average shortest path length $\langle L \rangle$, as is shown in Fig. 12(c).

B. Growth period ($\tau_1 < \tau < \tau_2$)

After the formation period, the square is full of small area domains (a little larger than minimum grid cell) as well as minimum grid cells. Therefore, as the network evolves for the further step, the unities between small area domains formed in the first period and those remaining minimum grid cells will dominate the evolving process, and thereby this period is named as the growth period of these small area domains. Generally, in this period, the area of domains increases steadily, as is shown in Fig. 12(d). In fact, the average maximum domain area of the networks in this period is close to 15, much larger than that of the first period.

At the same time, as is shown in Figs. 12(a) and 12(b), the increasing rates of the average degree and the average clustering coefficient will be both reduced due to the fact that there are considerable number of triangles in the network of this period, i.e., in such networks, statistically, more than one link will disappear when two nodes are united and the total increment of the clustering coefficient will also be much smaller than that in a lattice. Furthermore, after the first period, there are a large number of small area domains, as a result, the influence of the unity between a small area domain and a minimum grid cell on the average shortest path length is localized, so the decrease rate of the average shortest path length will also be reduced in this period, as is shown in Fig. 12(c).

C. Combination period ($\tau > \tau_2$)

After the growth period, there are more small area domains and several medium area domains are also formed, while the number of the minimum grid cells decrease ultimately, as a result, many of these small or medium area

domains will adjoin with each other. So a notable characteristic in this period is that large area domains appear by combining those adjoined small and medium area domains; accordingly, this period is named as combination period. Figure 12(d) shows that, in this period, the maximum domain area of the network increases very fast as the network evolves, i.e., from 24 at phase $\tau=0.72$ to 66 at phase $\tau=0.84$, and ultimately to 225 at phase $\tau=0.97$. Naturally, the existence of the large area countries, e.g., Russia and China, in the AEA continent may suggest that the AEA cluster is in its combination period.

Intuitively, more links will disappear when two larger area domains are combined, as a result, the appearance of the large area domains will finally largely decrease the average degree of the network, as is shown in Fig. 12(a). However, the appearance of the large area domains, on the other hand, will largely increase the compactness between different areas, i.e., in this period, the average clustering coefficient of the network increases even faster while its average shortest path length decreases faster than that in the growth period, as is shown in Figs. 12(b) and 12(c).

V. SUMMARY

In this paper, the giant component of the country neighborhood network (CNN), i.e., the Asia, Europe and Africa (AEA) cluster, is carefully analyzed. The structure of the CNN is of much sociological importance with the fact that natural population migration occurs frequently between neighbored countries, which could be partially confirmed by the network correlation of the population densities of countries in the AEA cluster. Then a geometrical model is proposed to explain its statistical properties, e.g., large average clustering coefficient, power-law domain area distribution, fractal domain borderlines, and so on. More interestingly, the network description of the AEA continent may provide a new statistical method to calculate the fractal dimension of its country borderlines by analyzing the relationship between the area of a country and the degree of the corresponding node, i.e., the near power-law country area-degree relationship of the AEA cluster with the exponent close to 1.7 may imply a fractal dimension close to 1.2 of country borderlines in the AEA continent. Generally, the network evolving process can be divided into three periods, defined as formation period, growth period, and combination period, and the existence of the large area countries, e.g., Russia and China, in the AEA continent may suggest that the AEA cluster is in its combination period.

However, many aspects of the model need to be improved in the future. For example, in order to provide a more general model, the complex geographical condition on the AEA continent, e.g., Africa is connected to Asia and Europe through a narrow chain, is not considered in this paper, as a result, the average shortest path length $\langle L \rangle$ predicted by the model is much smaller than that of the AEA cluster. Also the fact that, in the evolution history of countries, unbalanced neighbors are more likely to be united as one than balanced neighbors is also not expressed in the model, which results that the

network derived by the model has much stronger disassortativity than that of the AEA cluster. Besides, the influence of the dimension of the evolving space on the structural properties of the resulting network also belongs to our future works. Naturally, the network derived by the model in a higher dimensional space will for sure have a broader degree scaling, i.e., the model proposed in this paper would explain the power-law distributions more appropriately in a higher dimensional evolving space.

ACKNOWLEDGMENTS

We would like to thank all the members in our research group in the Department of Control Science and Engineering, Zhejiang University at Yuquan Campus, for the valuable discussion about the ideas presented in this paper. This work was supported by China Postdoctoral Science Foundation (Grant No. 20080441256) and the National 973 Program of China (Grant No. 2002CB312200).

-
- [1] A.-L. Barabási and R. Albert, *Science* **286**, 509 (1999).
 - [2] P. S. Dodds, R. Muhamad, and D. J. Watts, *Science* **301**, 827 (2003).
 - [3] M. Á. Serrano and M. Boguñá, *Phys. Rev. E* **68**, 015101(R) (2003).
 - [4] S.-H. Yook, H. Jeong, and A.-L. Barabási, *Proc. Natl. Acad. Sci. U.S.A.* **99**, 13382 (2002).
 - [5] R. Guimerà, S. Mossa, A. Turtschi, and L. A. N. Amaral, *Proc. Natl. Acad. Sci. U.S.A.* **102**, 7794 (2005).
 - [6] W. Li and X. Cai, *Phys. Rev. E* **69**, 046106 (2004).
 - [7] A.-L. Barabási and Z. N. Oltvai, *Nature (London)* **5**, 101 (2004).
 - [8] E. Ravasz, A. L. Somera, D. A. Mongru, Z. N. Oltvai, and A.-L. Barabási, *Science* **297**, 1551 (2002).
 - [9] S. Boccaletti, V. Latora, Y. Moreno, M. Chavez, and D.-U. Hwang, *Phys. Rep.* **424**, 175 (2006).
 - [10] L. D. F. Costa, F. A. Rodrigues, G. Travieso, and P. R. V. Boas, *Adv. Phys.* **56**, 167 (2007).
 - [11] D.-H. Kim, G. J. Rodgers, B. Kahng, and D. Kim, *Physica A* **351**, 671 (2005).
 - [12] Q. Xuan, Y. Li, and T.-J. Wu, *Phys. Rev. E* **73**, 036105 (2006).
 - [13] J. D. Noh, H.-C. Jeong, Y.-Y. Ahn, and H. Jeong, *Phys. Rev. E* **71**, 036131 (2005).
 - [14] Q. Xuan, Y. Li, and T.-J. Wu, *Physica A* **378**, 561 (2007).
 - [15] M. E. J. Newman, S. H. Strogatz, and D. J. Watts, *Phys. Rev. E* **64**, 026118 (2001).
 - [16] G. Caldarelli, A. Capocci, P. De Los Rios, and M. A. Munoz, *Phys. Rev. Lett.* **89**, 258702 (2002).
 - [17] Q. Xuan, Y. Li, and T.-J. Wu, *Chin. Phys. Lett.* **25**, 323 (2008).
 - [18] X.-H. Wang, S.-F. Wei, and L.-Z. Xu, *World Map (Xi'an Atlas Press, Xi'an, 2006)*.
 - [19] S.-W. Li, R.-F. Liu, L.-G. Chen, and X.-C. Zhou, *World Atlas (Geological Press, Beijing, 2005)*.
 - [20] H. J. Herrmann, G. Mantica, and D. Bessis, *Phys. Rev. Lett.* **65**, 3223 (1990).
 - [21] J. S. Andrade, H. J. Herrmann, R. F. S. Andrade, and L. R. da Silva, *Phys. Rev. Lett.* **94**, 018702 (2005).
 - [22] B. B. Mandelbrot, *The Fractal Geometry of Nature (W. H. Freeman and Co, Press, New York, 1983)*.
 - [23] R. O.-Saber and R. M. Murray, *IEEE Trans. Automat. Contr.* **49**, 1520 (2004).
 - [24] L.-E. Cederman, *Am. Polit. Sci. Rev.* **97**, 135 (2003).
 - [25] M. Mitzenmacher, *Internet Math.* **1**, 226 (2004).
 - [26] G.-Z. Luo, *Three Kingdoms (Shanghai Guji Press, Shanghai, 1998)*.
 - [27] Y. Zhao, *J. Hist. Med. Allied Sci.* **12**, 95 (2006).